

# Two-step estimators of high dimensional correlation matrices

Andrés García Medina\*

*Centro de Investigación en Matemáticas, Unidad Monterrey,  
Av. Alianza Centro 502, PIIT 66628, Apodaca, Nuevo León, México and  
Consejo Nacional de Ciencia y Tecnología, Av. Insurgentes Sur 1582,  
Col. Crédito Constructor 03940, Ciudad de México, México*

Salvatore Miccichè†

*Dipartimento di Fisica e Chimica Emilio Segrè, Università degli Studi di Palermo,  
Viale delle Scienze, Ed. 18, 90128, Palermo, Italy*

Rosario N. Mantegna‡

*Dipartimento di Fisica e Chimica Emilio Segrè, Università degli Studi di Palermo,  
Viale delle Scienze, Ed. 18, 90128, Palermo, Italy and  
Complexity Science Hub Vienna, Josefstädter Strasse 39, 1080 Vienna, Austria*

(Dated: January 2, 2023)

We investigate block diagonal and hierarchical nested stochastic multivariate Gaussian models by studying their sample cross-correlation matrix on high dimensions. By performing numerical simulations, we compare a filtered sample cross-correlation with the population cross-correlation matrices by using several rotationally invariant estimators (RIE) and hierarchical clustering estimators (HCE) under several loss functions. We show that at large but finite sample size, sample cross-correlation filtered by RIE estimators are often outperformed by HCE estimators for several of the loss functions. We also show that for block models and for hierarchically nested block models the best determination of the filtered sample cross-correlation is achieved by introducing two-step estimators combining state-of-the-art non-linear shrinkage models with hierarchical clustering estimators.

## I. INTRODUCTION

In recent years, many research areas deal with multivariate time series. Examples are physics, neuroscience, finance, climatology, genomics, etc. In all these research areas investigators perform  $n$  measurements of a system characterized by  $p$  variables therefore obtaining an observation matrix  $\mathbf{Y}$  of dimension  $p \times n$ . After standardization of the  $p$  series of  $n$  records, one can compute the  $p \times p$  sample cross-correlation matrix  $\mathbf{E}$ . Sample cross-correlation matrices computed from a finite set of multivariate data in general differ from the population cross-correlation matrix  $\mathbf{C}$  associated with the model generating multivariate data. Since the seminal work of Marcenko and Pastur [1] many studies have considered the spectral properties of sample cross-correlation matrices and have used these theoretical results to set up a null model useful to discriminate information that can be extracted from data, i.e., information not compatible with a null model, and information hard to be distinguished from noise, i. e., a null model, in empirical data [2].

Comparing sample and population cross-correlation requires the choice of a loss function, i.e., of a function specifying a penalty for an incorrect estimate from the underlying statistical model. In the literature, several loss

functions have been proposed and the choice of a specific one must be related to the specific problem considered. Most used loss functions are Frobenius loss, Stein loss, and Kullback-Leibler divergence.

In [3], the authors analytically demonstrate that the expected value of the Kullback-Leibler (KL) divergence of a sample correlation matrix concerning the population matrix does not depend on the reference model. The authors used the KL divergence to measure how informative the filtered correlation matrices are when applying spectral and hierarchical clustering techniques separately. The study performs simulations against factor model structures [4] and empirical studies with financial time series listed on US equity markets. As spectral techniques, the authors use two variations of methods known in the literature as the *clipping* technique. The clipping (also known as filtering or denoising in the econophysics community) technique was initially proposed in the work [5, 6] and later catalogued in the family of Rotationally Invariant Estimators (RIE) by [2]. In particular, the clipping technique is associated with the spiked covariance matrix model [7].

RIE models for estimating the covariance matrix have been known in the mathematical statistics community since Stein [8] proposed them under the name *rotation-equivariant* estimators. His idea was to keep the eigenvectors of the sample covariance matrix while shrinking its eigenvalues. They were proposed in the classical paradigm when the number of observations is much greater than the number of variables. Ledoit and Wolf have been promoting of these methods on the high-

---

\* andres.garcia@cimat.mx

† salvatore.micchiche@unipa.it

‡ rosario.mantegna@unipa.it

dimensional stage. In [9], they proposed an optimal linear shrinkage using Random Matrix Theory (RMT) concepts. Later on, in [10] proposed the first non-linear shrinkage model based on RMT and asymptotic theory. Their numerical implementation is given in [11]. On the other hand, Bun, Bouchaud, and Potters [2] suggest a different numerical approach that is easier to implement. Both are approximations of the same model. Finally, Ledoit and Wolf give a kernel-based solution that is essentially analytical and drastically improves the computation time by two orders of magnitude [12]. This solution is valid for general correlation structures but does not consider autocorrelations. Burda and Jarosz tackle the autocorrelation structure in a recent work [13] by using concepts of RMT and free probability.

The previous formulations lead to the consideration of non-linear shrinkage formulas to estimate the population eigenvalues from the empirical ones and reconstruct the correlation matrices using the empirical eigenvectors. As such, they belong to the RIE family of estimators. These non-linear shrinkage formulas are optimal with the Frobenius loss function. The problem of applying different loss functions is of current interest, as stated in [2], where they propose to quantify the information kept by the optimal RIE compared to other estimators and metrics analogously as the authors of [3, 14, 15] do with the classical RMT estimators or clipping techniques.

Although the subject has been analytically studied in [16], the conditions are very restrictive. They do not contemplate correlation matrix scenarios that capture the structure of financial markets, diagonal and nested hierarchical block matrices. Since there are no analytical results with similar assumptions, in this work we conduct a numerical analysis to understand the behaviour of different metrics for these correlation structures. In addition, we have included hierarchical clustering estimators for which there are no analytical comparisons. Our numerical results suggest to consider hypotheses that we hope can stimulate the development of new analytical results in the theory of random matrices and understanding of the structures of correlation matrices in financial markets in high dimensionality.

Specifically, we numerically analyze block diagonal and hierarchical nested models on high dimensions and compare their behaviour under several loss functions when applying RIE and hierarchical estimators. We are also introducing two-step estimators that combines state-of-the-art non-linear shrinkage models with hierarchical clustering estimators. These estimators outperform several of the most used estimators when the model of multivariate series is a block model or a hierarchically nested block model and when the statistical properties of records are Gaussian.

The paper is organized as follows. Section 2 describes the estimators proposed in this work. Section 3 introduces the loss functions used to evaluate the difference between filtered sample correlation and population correlation when applying each estimator. Section 4 gives the

specifications of the models studied. Section 5 shows the main results obtained. Section 6 analyzes and discusses the findings found.

## II. ESTIMATORS

For the sake of completeness, this section presents the estimators of the correlation matrix that we will use in our numerical analyses. These estimators can be grouped into three classes. The first ones belong to the RIE family, the second ones are of the hierarchical clustering type, and the third class combines both, which we denote as two-step estimators. It is important to emphasize that the first class of estimators is designed to deal with the estimation uncertainty inherent in the high-dimensional scenario when the number of variables is of the same order as the number of observations. The second class of estimators deal with the estimation uncertainty associated with the structure of the correlation blocks between variables. Therefore, it is focused on a better detection of the financial sectors. Finally, the third class of estimators deals with both types of noise.

### A. Rotationally Invariant Estimators (RIE)

The RIE has the property that the sample correlation matrix  $\mathbf{E}$  can be rotated by some orthogonal matrix  $\mathbf{O}$  and its estimation, denoted as  $\Xi$ , must be rotated in the same direction. Therefore,  $\Xi(\mathbf{E})$  can be diagonalized on the same basis as  $\mathbf{E}$  except for a fixed rotation  $\Omega$ . In this way,  $\Xi(\mathbf{E})$  has the same eigenvectors as  $\mathbf{E}$  and it is possible to write

$$\Xi(\mathbf{E}) = \sum_{i=1}^p \xi_i v_i v_i', \quad (1)$$

where  $v_i$  are the eigenvectors of  $\mathbf{E}$ , and  $\xi_i$  is a function of the eigenvalues  $[\lambda_j]_{j \in \{1, p\}}$  of  $\mathbf{E}$ .

A trivial example that satisfies this condition is the empirical correlation matrix  $\mathbf{E}$ . Then, a *naive estimator* is

$$\Xi^{naive}(\mathbf{E}) = \mathbf{E} \quad (2)$$

A more interesting estimator is the convex linear combination of the sample covariance matrix with the identity matrix, known as *linear shrinkage* and expressed as

$$\Xi^{linear} = \hat{\alpha} \mathbf{I} + (1 - \hat{\alpha}) \mathbf{E}, \quad (3)$$

where  $\mathbf{I}$  denotes the identity matrix and  $\hat{\alpha}$  is the optimal parameter  $\alpha$  that shrinks  $\mathbf{E}$  to  $\mathbf{I}$ . The asymptotically optimal  $\hat{\alpha}$  (as the number of observations and variables go to infinity together) with respect to the quadratic loss function is found to be [9]

$$\hat{\alpha} = \frac{\min\{\frac{1}{n} \sum_{i=1}^n \|x_i x_i' - \mathbf{E}\|_F^2, \|\mathbf{E} - \mathbf{I}\|_F^2\}}{\|\mathbf{E} - \mathbf{I}\|_F^2}, \quad (4)$$

where  $\|\cdot\|_F$  represents the Frobenius norm and  $x_i$  is the  $i$ -th column of  $\mathbf{E}$ .

A classical RMT filter is proposed in [5, 6] and is expressed as

$$\xi^{RMT} = \begin{cases} \bar{\lambda} & \text{if } \lambda_k < (1 + \sqrt{q})^2 \\ \lambda_k & \text{otherwise} \end{cases} \quad (5)$$

where  $\bar{\lambda}$  represents the average of the eigenvalues below the upper bound of the Marchenko-Pastur law. Then, the estimated correlation matrix is given by

$$\Xi^{RMT} = \sum_{i=1}^p \xi_i^{RMT} v_i v_i', \quad (6)$$

A nonlinear shrinkage formula of the RIE family to estimate the unbiased covariance matrix when  $\mathbf{C}$  has a general form is given by [10]

$$\xi_k^{LP} = \lim_{\epsilon \rightarrow 0^+} \frac{\lambda_k}{|1 - q + q\lambda_k G_E(\lambda_k - i\epsilon)|^2} \quad (7)$$

$$= \frac{\lambda_k}{|1 + u_k|^2} \quad (8)$$

$$= \frac{\lambda_k}{(\alpha_k + 1)^2 + \beta_k^2}, \quad (9)$$

where  $\lambda_k$  is an eigenvalue of  $\mathbf{E}$ ,  $G_E$  is the Stieltjes transform of  $\mathbf{E}$ , and since we are close to the real axis, the Sokhotski-Plemelj formula applies

$$u_k = qT_E(\lambda_k - i0^+) = \alpha_k + i\beta_k, \quad (10)$$

where  $T_E = zG_E(z) - 1$ ,  $\alpha_k = q(\pi\lambda_k h_E(\lambda_k) - 1)$ , and  $\beta_k = q\pi\lambda_k$ .  $\rho_E$  is the density of eigenvalues of  $\mathbf{E}$ , and  $h_E$  the Hilbert transform of  $\mathbf{E}$ . The corresponding estimated correlation matrix is given by the following expression:

$$\Xi^{LP} = \sum_{i=1}^p \xi_i^{LP} v_i v_i', \quad (11)$$

A recent proposal for non-linear shrinkage expression is due to Burda and Jarosz [13], who incorporate autocorrelation into data-generating processes through a matrix  $\mathbf{A}$ . The authors gave explicit solutions for some specific models of the Vector Autoregressive Moving Average (VARMA) family:

$$Y_{i,a} = \sum_{\beta=1}^{r_1} b_\beta Y_{i,a-\beta} + \sum_{\alpha=0}^{r_2} a_\alpha \epsilon_{i,a-\alpha}. \quad (12)$$

The key element to analytically incorporate autocorrelations is the  $\mathcal{S}$ -transform of the associated matrix of coefficients  $\mathbf{A}$ , which in principle, is not trivial to compute. Calculating  $\mathcal{S}$  requires some knowledge of the free probability [17, 18]. Burda and Jarosz explicitly solve the model for  $(r_1, r_2) \in \{(1, 1), (1, 0), (2, 0), (0, 1), (0, 2)\}$ . The nonlinear shrinkage formula has the general form

$$\xi_k^{BJ} = \frac{\lambda_k \text{Im}\{1/Z_A(u_k)\}}{\text{Im}\{u_k\}} \quad (13)$$

where  $Z_A$  is the  $\mathcal{Z}$ -transform of  $\mathbf{A}$ . Consequently, the optimal estimator in the Frobenius sense is:

$$\Xi^{BJ} = \sum_{i=1}^p \xi_i^{BJ} v_i v_i', \quad (14)$$

Notice that when  $A = \mathbf{I}$ , the  $\mathcal{S}$ -transform of  $A$  is given by

$$S_A(t) = \frac{t+1}{tZ_A(t)} = 1 \Rightarrow Z_A(t) = \frac{t+1}{t} \quad (15)$$

Then

$$\xi_k^{BJ} = \frac{\lambda_k \text{Im}\{1/Z_A(u_k)\}}{\text{Im}\{u_k\}} = \frac{\lambda_k}{(\alpha_k + 1)^2 + \beta_k^2}, \quad (16)$$

and we recover Eq. 9.

In particular, the combination of parameters  $a_0 = \sqrt{1 - b_1^2}$ ,  $b_1 = e^{-1/\tau}$ ,  $a_i = b_{i-1} = 0$  (for  $i > 1$ ) represents the exponential decay model for which  $Z_A$  is known analytically [19, 20]

$$Z_A(z) = \gamma + \sqrt{\gamma^2 - 1 + 1/z^2}, \quad (17)$$

where  $\gamma = \coth(1/\tau)$ .

A further estimator proposed from a data-driven approach employs the technique known as *moving window cross-validation* (mwcv) and is denoted as the oracle estimator [21]. It is important to mention that this estimator is an approximation of the state-of-the-art nonlinear shrinkage [22]. The expression to estimate the population eigenvalues is given by the expression:

$$\xi_i^{mwcv} = \frac{1}{K} \sum_{\mu}^{K-1} \langle \lambda_i^{train, \mu} | \mathbf{E}^{test, \mu} | \lambda_i^{train, \mu} \rangle, \quad (18)$$

where  $K = (T_{total} - T)/T_{out}$ . The idea is to set  $T$  observations as a train and  $T_{out}$  as a test in a moving window scenario of the entire sample sequence of length  $T_{total} = KT_{out} + T$ . Here,  $\lambda_i^{train, \mu}$  represents the eigenvalues of the training sample in window  $\mu$  and  $\mathbf{E}^{test, \mu}$  the test sample covariance matrix in window  $\mu$ .

$$\Xi^{mwcv} = \sum_{i=1}^p \xi_i^{mwcv} v_i v_i', \quad (19)$$

## B. Hierarchical clustering estimators

The hierarchical clustering estimator was proposed in [3]. Here, we restate the procedure with a different notation and a slight change in the way the dissimilarity matrix is constructed. The first step is to transform the correlation matrix  $\mathbf{E}$  into a dissimilarity matrix with  $i, j$  elements  $D_{ij} = 1 - E_{ij}$ . Then, apply the Average Linkage Clustering (ALCA) or the Single Linkage Clustering (SLCA) to  $\mathbf{D}$ . The third step consists of computing the *Cophenetic correlation* [23]  $\rho$  on the associated

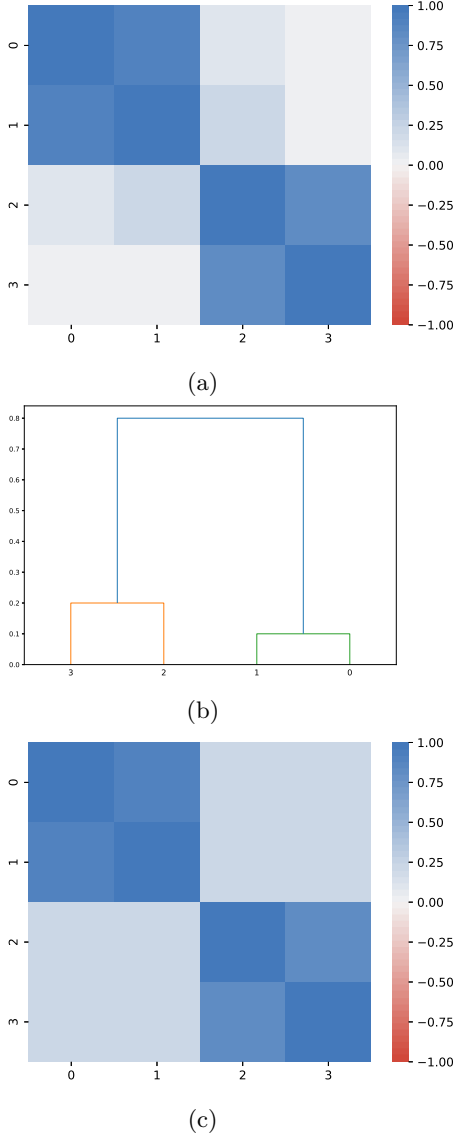


FIG. 1: The effect of applying the hierarchical clustering estimator under the SLCA approach to a  $4 \times 4$  matrix with a nested hierarchical structure. (a) represent an empirical matrix  $\mathbf{E}$ , (b) the associated dendrogram, and (c) the filtered correlation matrix  $\Xi(\mathbf{E})$ .

dendrogram. The next step is constructing a dissimilarity matrix as a function of  $\rho$ :  $\mathbf{D}(\rho)$ . Finally, the filtered correlation matrix is obtained by  $\Xi(E)_{ij} = 1 - D_{ij}(\rho)$ . Figure 1 shows the effect of applying the hierarchical clustering estimator under the SLCA approach to a  $4 \times 4$  matrix with a nested hierarchical structure. In the example, we show that the finer structures are filtered out using this procedure and that only strongest correlation blocks are preserved.

### C. Two-step estimators

Finally, here we introduce two-step estimators, which consist in applying as a first step a RIE estimator to deal with the statistical uncertainty due to high dimensionality. Once this type of uncertainty is eliminated, a hierarchical clustering-based estimator is applied as a second step to highlight block structure. In particular, we consider the following combination of estimators because they present very good performance

- 2-step (I):  $\Xi^{ALCA}(\Xi^{mwc}(\mathbf{E}))$
- 2-step (II):  $\Xi^{ALCA}(\Xi^{BJ}(\mathbf{E}))$
- 2-step (III):  $\Xi^{ALCA}(\Xi^{LP}(\mathbf{E}))$

### III. LOSS FUNCTIONS

To compare the effect of the different estimators on the correlation matrices, we use six different loss functions. The first of these is the Kullback-Leibler divergence. Let  $\mathbf{A}, \mathbf{B}$  be two square matrices of dimension  $p \times p$ , the KL divergence of Gaussian processes is given by [3]

$$K(\mathbf{A}, \mathbf{B}) = \frac{1}{2} [\log[\det(\mathbf{B}\mathbf{A}^{-1})] + \text{Tr}(\mathbf{B}^{-1}\mathbf{A}) - p] \quad (20)$$

we note that, under the assumption of Gaussianity,  $K(\mathbf{A}, \mathbf{B})$  is equivalent up to a factor to the inverse Stein's loss function.

The second metric is the inverse KL divergence or Stein's loss. This metric has the same expression as the KL divergence given above but applied on the inverse matrices:  $K(\mathbf{A}^{-1}, \mathbf{B}^{-1})$ . It is important to mention that the Stein's loss function  $\mathcal{L}^{Stein}$  is related to the inverse KL divergence by a scaling factor

$$\mathcal{L}^{Stein}(\mathbf{A}, \mathbf{B}) = \frac{1}{p} \text{Tr}(\mathbf{A}^{-1}\mathbf{B}) \quad (21)$$

$$-\frac{1}{p} \log[\det(\mathbf{A}^{-1}\mathbf{B})] - 1 = \frac{2}{p} K(\mathbf{A}^{-1}, \mathbf{B}^{-1}) \quad (22)$$

In this work, it is considered the scaled version to prevent the loss function from going to infinity with the matrix dimension, and both metrics (Stein's loss and inverse KL) are assumed to be indistinguishable. In [3] has been shown that the expected value of the KL divergence does not depend on the specific model under the Gaussian assumption. Consider two independent sample covariance matrices  $\mathbf{E}_1, \mathbf{E}_2$  coming from the parent population  $\mathbf{C}$ , the next scaled expectations are valid under Gaussian assumptions

$$\begin{aligned} \mathbb{E}[K(\mathbf{E}_1, \mathbf{E}_2)] &= \frac{p+1}{n-p-1} \\ \mathbb{E}[K(\mathbf{C}, \mathbf{E})] &= \frac{1}{p} \left[ p \log\left(\frac{2}{n}\right) + \sum_{t=n-p+1}^n \left( \frac{\Gamma'(t/2)}{\Gamma(t/2)} \right) + \frac{p(p+1)}{n-p-1} \right] \end{aligned} \quad (23)$$

where  $\Gamma(x)$  is the usual gamma function and  $\Gamma'(x)$  is the derivative of  $\Gamma(x)$ . We have scaled the metric by  $\frac{2}{p}$  to have an exact equivalence between Stein's loss and the KL divergence [24], yet the original result does not take this factor into account.

Moreover, the Frobenius norm is given by

$$F(\mathbf{A}, \mathbf{B}) = \frac{1}{p} \text{Tr}[(\mathbf{A} - \mathbf{B})(\mathbf{A} - \mathbf{B})'], \quad (24)$$

the corresponding inverse Frobenius is  $F(\mathbf{A}^{-1}, \mathbf{B}^{-1})$ .

An interesting metric in the framework of portfolio theory is the minimum-variance loss function [25]:

$$MV(\mathbf{A}, \mathbf{B}) = \frac{\text{Tr}(\mathbf{B}^{-1}\mathbf{A}\mathbf{B}^{-1})/p}{[\text{Tr}(\mathbf{B}^{-1})/p]^2} - \frac{1}{\text{Tr}(\mathbf{A}^{-1})/p} \quad (25)$$

The last metric is the symmetrized Stein's loss, a combination of Stein's loss and the inverse of Stein's loss.

$$SS(\mathbf{A}, \mathbf{B}) = \frac{1}{p} \text{Tr}(\mathbf{B}\mathbf{A}^{-1} + \mathbf{B}^{-1}\mathbf{A}) - 2. \quad (26)$$

#### IV. MODEL

We consider a multiplicative noise model with the following structure

$$\mathbf{Y} = \sqrt{\mathbf{C}}\mathbf{X} \quad (27)$$

$$\mathbf{E} = \frac{1}{n} \sqrt{\mathbf{C}}\mathbf{X}\mathbf{X}'\sqrt{\mathbf{C}} \quad (28)$$

where  $\mathbf{Y}$  is the  $p \times n$  data matrix,  $\mathbf{C}$  is the  $p \times p$  population cross-correlation matrix and  $X_{ij} \sim \mathcal{N}(0, 1)$ , that is, each element  $X_{ij}$  follows a standard Gaussian distribution. The correlation model  $\mathbf{C}$  is first constructed by the loading matrix  $\mathbf{L}$  as follows

$$\mathbf{L}_{kl} = \begin{cases} \gamma_{kl}, & \text{if } k = k(l), \dots, k(l + p_l) \\ 0, & \text{otherwise,} \end{cases} \quad (29)$$

where  $\mathbf{L}$  is the loading matrix of dimension  $p \times b$ ,  $k = 1, \dots, p$ ,  $l = 1, \dots, b$ ,  $p_l$  the size of each block  $l$ , being  $b$  the number of blocks ( $b \leq p$ ), and  $\{k(l), k(l + p_l)\}$  are the initial and last value of the given block  $l$ . Once defined  $\mathbf{L}$ , the population correlation matrix  $\mathbf{C}$  is obtained simply by the expressions

$$\mathbf{Q} = \mathbf{L}\mathbf{L}', \quad (30)$$

$$C_{ij} = \delta_{ij} + Q_{ij}(1 - \delta_{ij}), \quad (31)$$

where  $\delta_{ij}$  denotes the Kronecker delta. We have considered a block diagonal and hierarchical nested block matrix structure to model  $\mathbf{C}$ . The first model comprises 12 independent diagonal blocks, while the second model is constructed with 12 overlapped diagonal blocks. In particular, we consider a homogeneous specification of the loading factors  $\gamma_{kl} = \gamma = 0.3$ . In both cases, the block sizes  $p_l$  are heterogeneous as well as the initial and last values  $\{k(l), k(l + p_l)\}$ .

#### V. RESULTS

We generate  $m$  realizations of multivariate series of each model of  $\mathbf{C}$ . Each sample matrix  $\mathbf{E}$  is then computed and filtered by using estimators described in Section II. Subsequently, the performance of the estimator is measured through the six loss functions described in section III. It is important to mention that some estimators produce pseudo-correlation matrices. Thus, the transformation  $\hat{\Xi}_{ij} = \frac{\Xi_{ij}}{\Xi_{ii}\Xi_{jj}}$  was applied to each of the estimated matrices  $\Xi$  to ensure that the results were comparable. Figure 2 shows a graphical representation of the two models accompanied by a realization of the process for  $p = 100, n = 200$ . It can be seen that sample matrices show statistical uncertainty because the number of observations and the number of variables are finite. This noise occurs naturally when we study cross-correlations of a large number of variables with a limited number of record. This condition is quite common in many research fields. For example, practitioners in finance prefer high dimensional setting, i.e.  $p \sim n$ , to avoid non-stationary effects or structural changes in return series of assets traded in financial markets.

Figures 3 and 4 show the behaviour of the average loss functions over  $m = 1000$  realizations and dimensions  $p = 100, n = 200$  for the block diagonal model and hierarchical nested model, respectively. Panels from (a) to (f) show  $\langle \mathcal{L}(\mathbf{C}, \Xi_i) \rangle$  vs.  $\langle \mathcal{L}(\Xi_i, \Xi_j) \rangle$ . We denote by  $\mathcal{L}$  each of the loss functions (KL divergence, Frobenius, etc.),  $\langle \cdot \rangle$  represents the average, and  $\Xi$  represents the filtered correlation matrix under each of the filtering strategies described in Section II. In the case of the  $\Xi^{mucv}$  estimator, we set  $T_{total} = 10T$  and  $T_{out} = T = n$ .

Our simulations confirm that  $\langle KL(\mathbf{C}, \Xi_i^{naive}) \rangle$  is in agreement with the theoretical limits of the KL divergence given by eqs. 23 (represented by the orange cross-ticker in the panels). The inset shows a zoom-in on the dynamics of the loss functions near the origin. The continuous black line shows the behaviour of the linear shrinkage estimator when the  $\alpha$  parameter varies from 1 to zero. Likewise, the solid grey line represents the RMT estimator when the number of eigenvalues  $\lambda$  that are kept in the filtering procedure varies from 1 to  $p$ . In both cases, the magnitude of their markers represents the standard deviation. The lower left corner corresponds to the case where we have kept only the signal associated with the largest eigenvalue and  $\alpha = 1$ . The upper right corner corresponds to the case where we have kept signals associated with all eigenvalues or signals and  $\alpha = 0$ , so the estimator is identically the empirical correlation matrix  $\mathbf{E}$ . In these curves, we are comparing the value that minimizes the loss function given the stability level of the estimators.

In the block diagonal model (see Figure 3), the curves' behaviour is monotonically increasing almost for every value, except very near the origin. Moreover, the optimal value given in equation (4) for the lin-

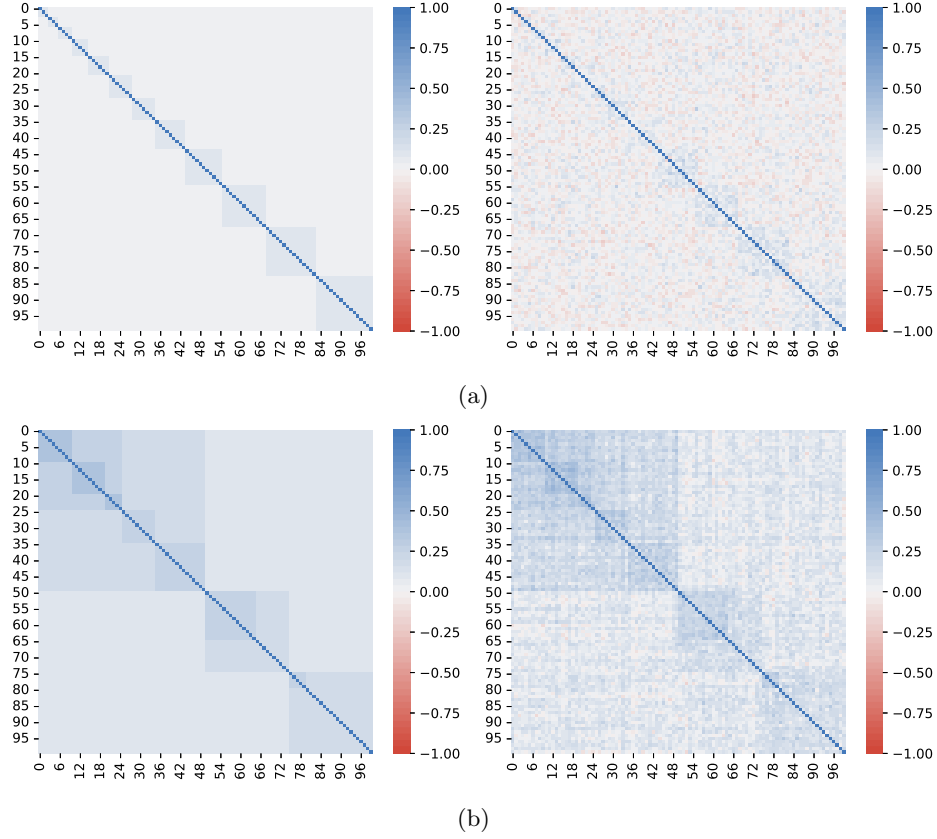


FIG. 2: (a) Block diagonal model. (b) Hierarchical nested model. The left figures are the population correlation matrix, and the right represents a single realization of such processes for dimensions  $p = 100, n = 200$ .

ear shrinkage is near the numerical minimum value of  $\Xi^{linear}(\alpha)$  (black curves) for all metrics. Particularly, the expression (4) is in agreement to the  $\alpha$  that minimizes  $\langle \mathcal{F}(\mathbf{C}, \Xi^{Linear}(\alpha)) \rangle$  (Figure 3c). This agreement is expected because expression (4) is optimized with respect to Frobenius loss [9].

In contrast, the curves of the hierarchical nested model (see Figure 4) are monotonically increasing only relatively far from the origin. Surprisingly, the RMT filter approximately coincides with the numerical minimum of  $\langle \mathcal{F}(\mathbf{C}, \Xi^{RMT}(\lambda)) \rangle$  (grey curves) for almost every metric. Thus, the Marchenko-Pastur bound effectively gives us the number of optimal signals to preserve in the hierarchical nested model. Nevertheless, the optimal value of the linear shrinkage is far from the numerical minimum value (black curves) in most cases. It only coincides with the Frobenius loss (Figure 4c) as should be.

The most notable change between the block diagonal and hierarchical nested model is about the Frobenius metric (see Figures 3c and 4c). In the latter, the behaviour of the linear shrinkage estimator as the  $\alpha$  parameter decreases is mostly monotonically decreasing. In addition, the estimators show greater instability since they reach their optimum value far from the origin to the x-axis.

Tables I and II summarize the performance of esti-

mators in terms of  $\langle \mathcal{L}(\mathbf{C}, \Xi_i) \rangle$  for the block diagonal model and the hierarchical nested model considering the average over  $m = 1000$  realizations and dimensions  $p = 100, n = 200$ . The standard deviations  $\sigma[\mathcal{L}(\mathbf{C}, \Xi_i)]$  of each estimator  $\Xi$  in relation to the loss function  $\mathcal{L}$  are shown in tables V and VI in Appendix A.

Table I shows that for the block diagonal model, the 2-step (III) estimator minimizes all the loss functions. In other words, the best strategy is to apply the  $\Xi^{LP}$  estimator followed by the ALCA filter. The second best option is the 2-step (III) estimator, which implies applying the estimator  $\Xi^{mwc}$  followed again by the ALCA filter. Notably, in third place, and very close to the minimum values of the two-step estimators mentioned above, are the results of simply applying the strategy  $\Xi^{mwc}$ . In contrast, the 2-step (II) and  $\Xi^{BJ}$  estimators are far from being to have the best performance as they should. It has been assumed in these estimators that the variables present autocorrelation with exponential decay when in reality, the simulations are generated with independent and identical distributed (i.i.d.) random variables.

The results for the nested hierarchical model are similar for the two best performances (see Table II). The exception concerns the Frobenius metric, where now the 2-step estimator (I) improves the performance of the 2-step estimator (III) and moves it to third place, with

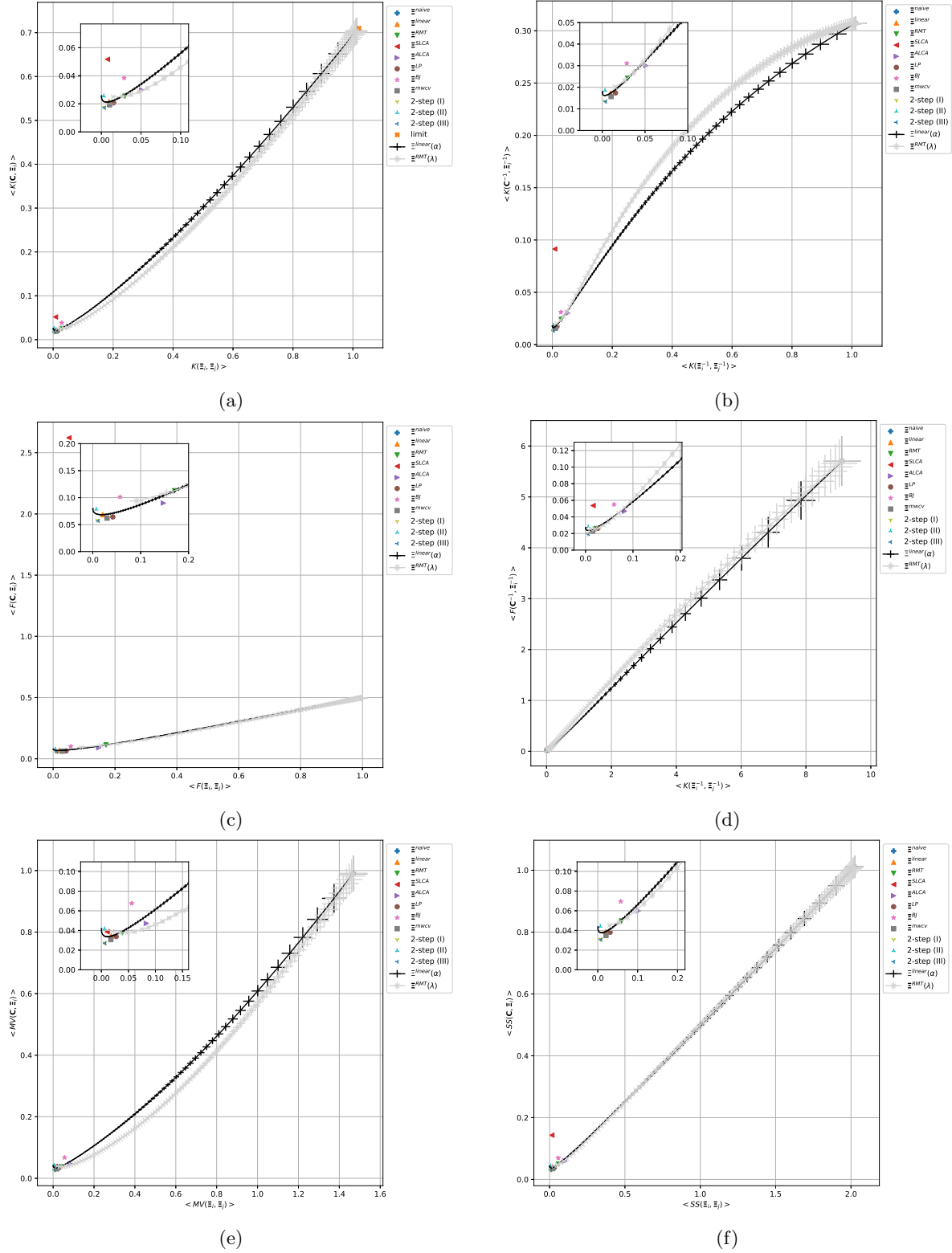


FIG. 3: Average loss functions over  $m = 1000$  realizations for the block diagonal model of dimensions  $p = 100, n = 200$ . (a)  $\langle K(\mathbf{C}, \Xi_i) \rangle$  vs.  $\langle K(\Xi_i, \Xi_j) \rangle$ , where the orange cross tickers represent the theoretical limits given by eqs. 23. (b)  $\langle K(\mathbf{C}^{-1}, \Xi_i^{-1}) \rangle$  vs.  $\langle K(\Xi_i^{-1}, \Xi_j^{-1}) \rangle$ . (c)  $\langle F(\mathbf{C}, \Xi_i) \rangle$  vs.  $\langle F(\Xi_i, \Xi_j) \rangle$ . (d)  $\langle F(\mathbf{C}^{-1}, \Xi_i^{-1}) \rangle$  vs.  $\langle F(\Xi_i^{-1}, \Xi_j^{-1}) \rangle$ . (e)  $\langle MV(\mathbf{C}, \Xi_i) \rangle$  vs.  $\langle MV(\Xi_i, \Xi_j) \rangle$ . (f)  $\langle SS(\mathbf{C}, \Xi_i) \rangle$  vs.  $\langle SS(\Xi_i, \Xi_j) \rangle$ . The inset shows a zoom-in on the dynamics of the loss functions near the origin.

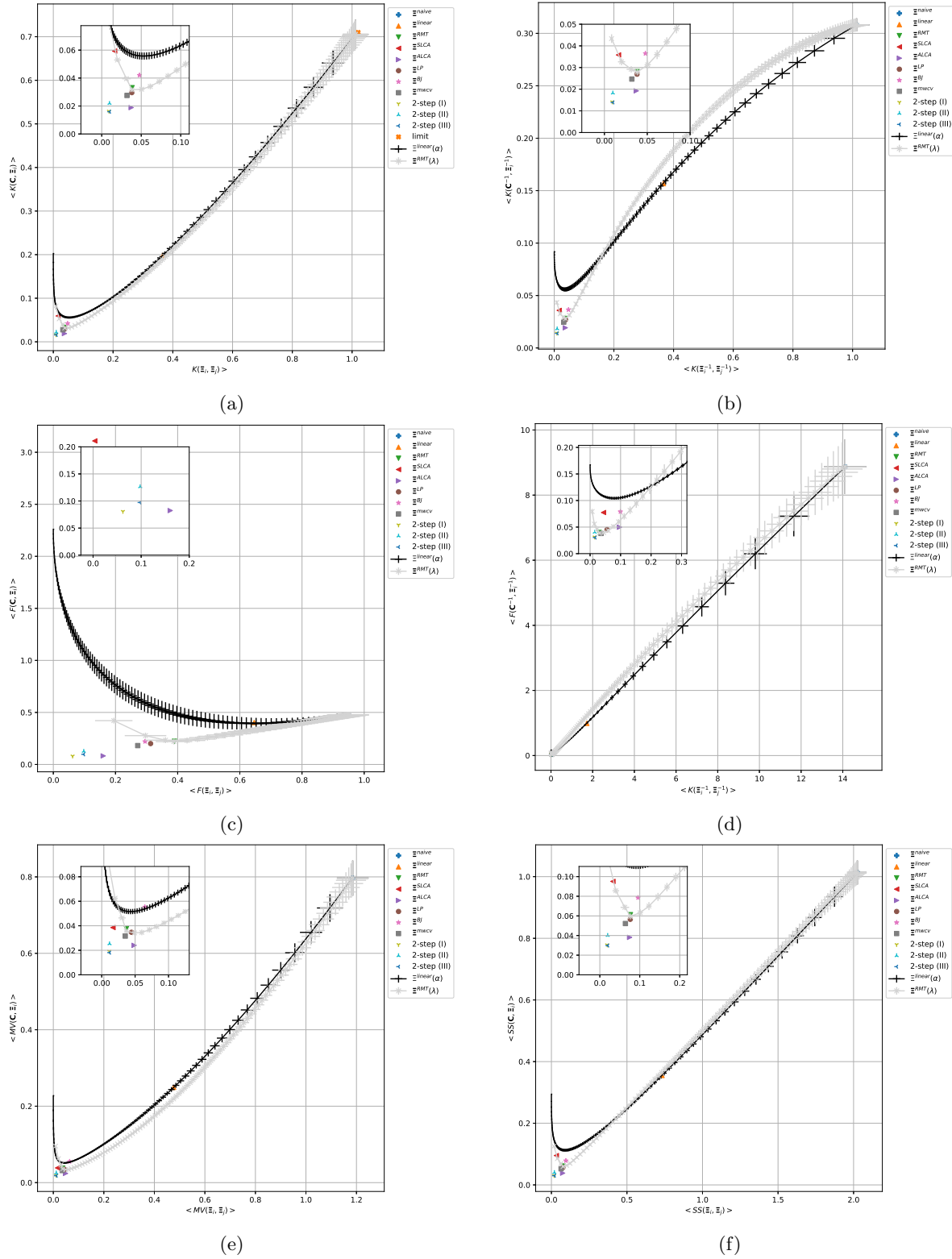


FIG. 4: Average loss functions over  $m = 1000$  realizations for the hierarchical nested model of dimensions  $p = 100, n = 200$ . (a)  $\langle K(\mathbf{C}, \Xi_i) \rangle$  vs.  $\langle K(\Xi_i, \Xi_j) \rangle$ , where the orange cross tickers represent the theoretical limits given by eqs. 23. (b)  $\langle K(\mathbf{C}^{-1}, \Xi_i^{-1}) \rangle$  vs.  $\langle K(\Xi_i^{-1}, \Xi_j^{-1}) \rangle$ . (c)  $\langle F(\mathbf{C}, \Xi_i) \rangle$  vs.  $\langle F(\Xi_i, \Xi_j) \rangle$ . (d)  $\langle F(\mathbf{C}^{-1}, \Xi_i^{-1}) \rangle$  vs.  $\langle F(\Xi_i^{-1}, \Xi_j^{-1}) \rangle$ . (e)  $\langle MV(\mathbf{C}, \Xi_i) \rangle$  vs.  $\langle MV(\Xi_i, \Xi_j) \rangle$ . (f)  $\langle SS(\mathbf{C}, \Xi_i) \rangle$  vs.  $\langle SS(\Xi_i, \Xi_j) \rangle$ . The inset shows a zoom-in on the dynamics of the loss functions near the origin.



TABLE I: Block diagonal model. Performance of estimators in terms of  $\langle \mathcal{L}(\mathbf{C}, \mathbf{\Xi}_i) \rangle$ , where  $\mathcal{L}$  denotes the loss function and  $\langle \cdot \rangle$  represents the average over the realizations of  $m = 1000$  and considering dimensions  $p = 100, n = 200$ .

	$\langle K(\mathbf{C}, \mathbf{\Xi}_i) \rangle$	$\langle K(\mathbf{C}^{-1}, \mathbf{\Xi}_i^{-1}) \rangle$	$\langle F(\mathbf{C}, \mathbf{\Xi}_i) \rangle$	$\langle F(\mathbf{C}^{-1}, \mathbf{\Xi}_i^{-1}) \rangle$	$\langle MV(\mathbf{C}, \mathbf{\Xi}_i) \rangle$	$\langle SS(\mathbf{C}, \mathbf{\Xi}_i) \rangle$
$\mathbf{\Xi}^{naive}$	0.703796	0.307311	0.496418	5.707239	0.990079	1.011107
$\mathbf{\Xi}^{linear}$	0.021526	0.017285	0.068648	0.025835	0.034452	0.038811
$\mathbf{\Xi}^{RMT}$	0.025472	0.024150	0.112820	0.025965	0.037611	0.049622
$\mathbf{\Xi}^{SLCA}$	0.051730	0.091388	2.622250	0.053663	0.038588	0.143118
$\mathbf{\Xi}^{ALCA}$	0.029854	0.030047	0.089948	0.046845	0.047245	0.059901
$\mathbf{\Xi}^{LP}$	0.020703	0.017400	0.064288	0.026265	0.033815	0.038103
$\mathbf{\Xi}^{BJ}$	0.038435	0.031078	0.101099	0.054970	0.067608	0.069513
$\mathbf{\Xi}^{mwcv}$	0.019308	0.015696	0.062019	0.022480	0.030723	0.035004
2-step (I)	0.017560	0.013539	0.058023	0.019606	0.027446	0.031099
2-step (II)	0.025519	0.018531	0.078456	0.028014	0.041655	0.044050
2-step (III)	<b>0.017230</b>	<b>0.013388</b>	<b>0.056831</b>	<b>0.019357</b>	<b>0.026947</b>	<b>0.030618</b>

TABLE II: Hierarchical nested model. Performance of estimators in terms of  $\langle \mathcal{L}(\mathbf{C}, \mathbf{\Xi}_i) \rangle$ , where  $\mathcal{L}$  denotes the loss function and  $\langle \cdot \rangle$  represents the average over the realizations of  $m = 1000$  and considering dimensions  $p = 100, n = 200$ .

	$\langle K(\mathbf{C}, \mathbf{\Xi}_i) \rangle$	$\langle K(\mathbf{C}^{-1}, \mathbf{\Xi}_i^{-1}) \rangle$	$\langle F(\mathbf{C}, \mathbf{\Xi}_i) \rangle$	$\langle F(\mathbf{C}^{-1}, \mathbf{\Xi}_i^{-1}) \rangle$	$\langle MV(\mathbf{C}, \mathbf{\Xi}_i) \rangle$	$\langle SS(\mathbf{C}, \mathbf{\Xi}_i) \rangle$
$\mathbf{\Xi}^{naive}$	0.705407	0.308104	0.476403	8.870820	0.796781	1.013511
$\mathbf{\Xi}^{linear}$	0.198429	0.156705	0.403202	0.989426	0.249332	0.355134
$\mathbf{\Xi}^{RMT}$	0.033107	0.028109	0.222649	0.039797	0.037707	0.061216
$\mathbf{\Xi}^{SLCA}$	0.059317	0.035824	3.109042	0.077423	0.038548	0.095141
$\mathbf{\Xi}^{ALCA}$	0.018876	0.019247	0.082322	0.049819	0.024047	0.038123
$\mathbf{\Xi}^{LP}$	0.029577	0.026931	0.200729	0.045210	0.034692	0.056508
$\mathbf{\Xi}^{BJ}$	0.042077	0.036511	0.220701	0.079080	0.055354	0.078588
$\mathbf{\Xi}^{mwcv}$	0.027548	0.024680	0.181307	0.038085	0.031579	0.052228
2-step (I)	0.016287	0.014133	<b>0.080718</b>	0.031280	0.019093	0.030420
2-step (II)	0.021883	0.018226	0.126338	0.040388	0.025320	0.040109
2-step (III)	<b>0.015920</b>	<b>0.013896</b>	0.097237	<b>0.030353</b>	<b>0.018104</b>	<b>0.029816</b>

the ALCA estimator having the second-best performance against this metric. This latter estimator turn shifts  $\mathbf{\Xi}^{mwcv}$  to obtain the third-best performance about the KL divergence, the MV, and SS loss functions. Only with the inverse Frobenius metric, the estimator  $\mathbf{\Xi}^{mwcv}$  obtains the third place. Finally, and surprisingly, the 2-step(II) estimator obtains the third-best performance against the inverse KL divergence.

Given that the estimators of random matrices and free probability are valid asymptotically, that is, when  $p, n \rightarrow \infty$ , we are interested in verifying that the results are not biased due to the finite dimensions. For this purpose, we have increased both dimensions by one order of magnitude and applied the same methodology. Table III and IV summarize the performance of estimators in terms of  $\langle \mathcal{L}(\mathbf{C}, \mathbf{\Xi}_i) \rangle$  for the block diagonal model and the hierarchical nested model considering the average over  $m = 100$  realizations and dimensions  $p = 1000, n = 2000$ . The standard deviations  $\sigma[\mathcal{L}(\mathbf{C}, \mathbf{\Xi}_i)]$  of each estimator  $\mathbf{\Xi}$  and the loss function  $\mathcal{L}$  are shown in tables VII and VIII of Appendix A. In this larger dimension scenario, we have reduced the number of realizations of the process over which the metrics are averaged since the computation time increases considerably. For example, the

hierarchical nested model lasted 72131.72 seconds in an Intel (R)Xeon(R) Gold 6254 CPU @ 3.10GHz 8 cores.

In the case of the high-dimensional block diagonal model, the three best performances are obtained by the 2-step (I), 2-step(III), and 2-step(II) estimators for almost all the metrics, respectively. The only exception is with the Frobenius metric, where the ALCA estimator is the one that obtains the minimum, followed by the 2-step(I) and 2-step(III) estimators, respectively. In the case of the hierarchical nested model, a similar ranking to the dominant one in the previous case is presented for the KL divergence, the inverse KL divergence, and the loss function SS. That is, in relation to these metrics, we have that the three best performances are obtained by the 2-step (I), 2-step(III), and 2-step(II), in the given order. Concerning the Frobenius loss function, the best performance is obtained by the ALCA estimator, for the inverse Frobenius the RMT estimator has the best performance whereas for the MV loss function the SLCA estimator gives the best performance. The second and third places alternate between the 2-step(I), 2-step(III), and even the  $\mathbf{\Xi}^{mwcv}$  estimator. The fact that hierarchical clustering estimators give us good performance is explained by the fact that the blocks become sharper as the

TABLE III: Block diagonal model. Performance of estimators in terms of  $\langle \mathcal{L}(\mathbf{C}, \mathbf{\Xi}_i) \rangle$ , where  $\mathcal{L}$  denotes the loss function and  $\langle \cdot \rangle$  represents the average of the realizations  $m = 100$  and considering the dimensions  $p = 1000, n = 2000$ .

	$\langle K(\mathbf{C}, \mathbf{\Xi}_i) \rangle$	$\langle K(\mathbf{C}^{-1}, \mathbf{\Xi}_i^{-1}) \rangle$	$\langle F(\mathbf{C}, \mathbf{\Xi}_i) \rangle$	$\langle F(\mathbf{C}^{-1}, \mathbf{\Xi}_i^{-1}) \rangle$	$\langle MV(\mathbf{C}, \mathbf{\Xi}_i) \rangle$	$\langle SS(\mathbf{C}, \mathbf{\Xi}_i) \rangle$
$\mathbf{\Xi}^{naive}$	0.694074	0.306877	0.498751	5.946251	0.922070	1.000951
$\mathbf{\Xi}^{linear}$	0.103291	0.093667	0.316267	0.295554	0.158213	0.196958
$\mathbf{\Xi}^{RMT}$	0.005670	0.006042	0.097030	0.002074	0.005873	0.011712
$\mathbf{\Xi}^{SLCA}$	0.007180	0.011587	7.831934	0.004538	0.002504	0.018767
$\mathbf{\Xi}^{ALCA}$	0.002403	0.002558	<b>0.009010</b>	0.005308	0.004083	0.004961
$\mathbf{\Xi}^{LP}$	0.005627	0.005294	0.085917	0.002439	0.006170	0.010921
$\mathbf{\Xi}^{BJ}$	0.033888	0.029660	0.124739	0.081555	0.061103	0.063549
$\mathbf{\Xi}^{mwcw}$	0.005459	0.005117	0.085041	0.002062	0.005879	0.010576
2-step (I)	<b>0.000760</b>	<b>0.000812</b>	0.016754	<b>0.000924</b>	<b>0.000799</b>	<b>0.001572</b>
2-step (II)	0.000987	0.000979	0.023769	0.001213	0.000991	0.001967
2-step (III)	0.000774	0.000823	0.017304	0.000936	0.000812	0.001597

TABLE IV: Hierarchical nested model. Performance of estimators in terms of  $\langle \mathcal{L}(\mathbf{C}, \mathbf{\Xi}_i) \rangle$ , where  $\mathcal{L}$  denotes the loss function and  $\langle \cdot \rangle$  represents the average of the realizations  $m = 100$  and considering the dimensions  $p = 1000, n = 2000$ .

	$\langle K(\mathbf{C}, \mathbf{\Xi}_i) \rangle$	$\langle K(\mathbf{C}^{-1}, \mathbf{\Xi}_i^{-1}) \rangle$	$\langle F(\mathbf{C}, \mathbf{\Xi}_i) \rangle$	$\langle F(\mathbf{C}^{-1}, \mathbf{\Xi}_i^{-1}) \rangle$	$\langle MV(\mathbf{C}, \mathbf{\Xi}_i) \rangle$	$\langle SS(\mathbf{C}, \mathbf{\Xi}_i) \rangle$
$\mathbf{\Xi}^{naive}$	0.694047	0.306968	0.478731	9.332066	0.736720	1.001015
$\mathbf{\Xi}^{linear}$	0.563801	0.279749	0.471146	6.363615	0.596513	0.843550
$\mathbf{\Xi}^{RMT}$	0.004670	0.004760	0.272674	<b>0.003190</b>	0.004008	0.009430
$\mathbf{\Xi}^{SLCA}$	0.004309	0.003766	7.442682	0.009240	<b>0.001409</b>	0.008075
$\mathbf{\Xi}^{ALCA}$	0.002896	0.003214	<b>0.040023</b>	0.009521	0.003738	0.006110
$\mathbf{\Xi}^{LP}$	0.005001	0.004839	0.265075	0.004736	0.004519	0.009840
$\mathbf{\Xi}^{BJ}$	0.029186	0.026273	0.332866	0.105884	0.042313	0.055460
$\mathbf{\Xi}^{mwcw}$	0.004775	0.004602	0.249636	0.003996	0.004215	0.009378
2-step (I)	<b>0.001436</b>	<b>0.001664</b>	0.094165	0.004090	0.001526	<b>0.003100</b>
2-step (II)	0.001673	0.001837	0.155693	0.005173	0.001804	0.003510
2-step (III)	0.001438	0.001665	0.108579	0.004069	0.001515	0.003103

dimensions increase since the number of blocks remains constant. An interesting fact is that the classic RMT filter obtains the best performance in one of the studied scenarios. The RMT estimator performs better than linear shrinkage because the latter dilutes the noise at the expense of diluting some of the signals as well [26]. A similar phenomenon may be presented in the non-linear shrinkage models.

## VI. DISCUSSION

In principle, one would expect that asymptotic estimators based on random matrices and free probability perform better as the dimension of the correlation matrix increases. However, we have found cases where the  $\mathbf{\Xi}^{ALCA}$  estimator shows better performance than the RIE estimators, even at  $p = 1000$ . This behaviour can be explained due to the assumptions of the semi-analytical solution of the non-linear shrinkage function proposed by Ledoit and Wolf. Their expression was also used in the Burda and Jarosz approach and in this analysis. The central assumption of the solution is the existence of a compact interval. It should contain all the eigenvalues as

the matrix dimensions tend to infinity. In other words, the eigenvalues should not grow with the dimension to converge to a well-defined density.

However, diagonal block and hierarchical nested models have one eigenvalue that grows with the dimension of each of their blocks (see appendix B). That is, a model of  $k$  blocks has  $k$  unbounded eigenvalues, which violates the assumptions of the asymptotic results of the RIE solutions. More precisely, the expressions in Eqs. 9, 16 are correct and valid as long as  $p, n \rightarrow \infty$ . What is problematic is the kernel approximation of the density  $\rho_E$  and the Hilbert transform  $h_E$  since they do not converge for our block structure models. Hence, our models violate this principle, which could be why RIE techniques do not work as well as  $\mathbf{\Xi}^{ALCA}$  for some loss functions and values of  $p$  and  $n$  dimensions.

The semi-analytical solution given in Ref. [16], has been tested through a Monte Carlo simulation where 20% of the population eigenvalues are equal to 1, 40% are equal to 3, and 40% is equal to 10. The authors argue that this diagonal model, originally introduced in [27], with three different (but finite) eigenvalues, is already complicated enough. In their population covariance model, they use a condition number of 10. In our

case, the block diagonal model has condition numbers of 5.25 and 43.5 for dimensions  $p = 100, 1000$ , respectively. In comparison, the hierarchical nested model has condition numbers of 23.18 and 75.79 for dimensions  $p = 100, 1000$ , respectively. Therefore, our model even represents more unstable cases in the sense that a slight disturbance in the inputs significantly modifies the outputs. Particularly important to estimate the inverse of the correlation matrix, which is the main ingredient in the optimisation of investment portfolios. Nevertheless, the arrow model [24], where an eigenvalue grows with dimension, shows signs of using a numerical estimation technique of eq. 9, which is radically different from the kernels approximation. Although, the nested hierarchical model has  $k$  eigenvalues, which grow with the dimension of each of the  $k$  nested blocks. Consequently, the theoretical optimality of the RIE estimators is even more complicated. In this sense, our contribution is to show, under numerical experimentation, that a hierarchical filter is adequate in this type of model. We hope these results motivate searching for theoretical foundations within the community of random matrices and asymptotic theory in future work.

On the other hand, the excellent performance of the data-driven estimator  $\Xi^{mwc}$  is notable. The authors of [22] proved that it is possible to approximate the optimal RIE estimator  $\xi(\lambda) = l$  (the true eigenvalues) by overlapping the eigenvectors of two different realisations of the same population covariance matrix  $\Sigma$ . The test sample covariance matrix can be rank-deficient, i.e.,  $n = T_{out} < p$ . Intuitively, the superposition of the training and testing eigenvectors helps estimate the empirical eigenvalues. As if rotating them into the test direction unveils their true value. This evidence opens the door to considering other types of non-linear shrinkage  $\xi(\lambda)$  under the RIE approach. An interesting future work is to consider statistical learning models to shape the function  $\xi(\lambda)$  and take into account the complex stylised fact of hierarchical block structures in the financial correlation matrices under more general distributional assumptions.

It is important to mention that the non-linear shrinkage functions  $\Xi^{LP}$  and  $\Xi^{BJ}$  are optimal concerning the Frobenius loss function. Future work goes in the direction of analysing the performance of the block diagonal and hierarchical nested models under a non-linear shrinkage formula optimised having as a target the loss function used to evaluate their performance and in the spirit of the proposed expressions in [16, 24, 28].

## ACKNOWLEDGMENTS

S.M. and R.N.M. acknowledge financial support by the MIUR PRIN project 2017WZFTZP, Stochastic forecasting in complex systems. A.G.M. acknowledge financial support by Consejo Nacional de Ciencia y Tecnología (CONACYT, Mexico) through fund FOSEC SEP-INVESTIGACION BASICA (Grant No. A1-S-43514).

## Appendix A

Tables V, VI, VII, and VIII show the standard deviations  $\sigma[\mathcal{L}(\mathbf{C}, \Xi_i)]$  for each estimator  $\Xi$  and loss function  $\mathcal{L}$  of tables I, II, III, and IV, respectively.

## Appendix B

### 1. Definitions and theorems

The following definitions and theorems have been extracted from [29] and are the basis for our derivations of the largest eigenvalues of the diagonal block and hierarchical nested models in the next subsection B 2.

**Definition 1** Let  $\mathbf{A} = [a_{ij}]$  be an  $n \times n$  complex matrix with eigenvalues  $\lambda_i, 1 \leq i \leq n$ . Then,

$$\rho(\mathbf{A}) := \max_{1 \leq i \leq n} |\lambda_i| \quad (\text{B1})$$

is the spectral radius of the matrix  $\mathbf{A}$ .

**Definition 2** For  $n \geq 2$ , an  $n \times n$  complex matrix  $\mathbf{A}$  is reducible if there exists a  $n \times n$  permutation matrix  $P$  such that

$$PAP' = \begin{pmatrix} A_{11} & A_{12} \\ O & A_{22} \end{pmatrix} \quad (\text{B2})$$

where  $A_{11}$  is an  $r \times r$  submatrix and  $A_{22}$  is an  $(n - r) \times (n - r)$  submatrix, where  $1 \leq r < n$ . If no such permutation matrix exists, then  $\mathbf{A}$  is irreducible. If  $\mathbf{A}$  is a  $1 \times 1$  complex matrix, then  $\mathbf{A}$  is irreducible if its single entry is nonzero, and reducible otherwise.

**Definition 3** A directed graph with  $n$  nodes is strongly connected if, for any pair  $(P_i, P_j)$  of nodes, with  $1 \leq i, j \leq n$ , there exists a directed path, consisting of abutting directed arcs

$$\overrightarrow{P_i P_1}, \overrightarrow{P_1 P_2}, \dots, \overrightarrow{P_{r-1} P_r}, \quad (\text{B3})$$

connecting  $P_i$  to  $P_j$ . (We shall say that this path has length  $r$ ).

**Theorem 1** An  $n \times n$  complex matrix  $\mathbf{A}$  is irreducible if and only if its directed graph  $G(\mathbf{A})$  is strongly connected.

**Definition 4** Let  $\mathbf{A} = [a_{ij}]$  and  $\mathbf{B} = [b_{ij}]$  be two real  $n \times r$  matrices. Then,  $\mathbf{A} \geq \mathbf{B}$  ( $\mathbf{A} > \mathbf{B}$ ) if  $a_{ij} \geq b_{ij}$  ( $a_{ij} > b_{ij}$ ) for all  $1 \leq i \leq n, 1 \leq j \leq r$ . If  $O$  is the null matrix and  $\mathbf{A} \geq O$  ( $\mathbf{A} > O$ ), we say that  $\mathbf{A}$  is a nonnegative (positive) matrix. Finally, if  $\mathbf{B} = [b_{ij}]$  is an arbitrary complex  $n \times r$  matrix, then  $|\mathbf{B}|$  denotes the nonnegative matrix with entries  $|b_{ij}|$ .

TABLE V: Standard deviation of table I

	$\sigma[K(\mathbf{C}, \Xi_i)]$	$\sigma[K(\mathbf{C}^{-1}, \Xi_i^{-1})]$	$\sigma[F(\mathbf{C}, \Xi_i)]$	$\sigma[F(\mathbf{C}^{-1}, \Xi_i^{-1})]$	$\sigma[MV(\mathbf{C}, \Xi_i)]$	$\sigma[SS(\mathbf{C}, \Xi_i)]$
$\Xi^{naive}$	0.029525	0.006198	0.010618	0.484784	0.057313	0.035151
$\Xi^{linear}$	0.000483	0.000653	0.001322	0.001266	0.000917	0.001014
$\Xi^{RMT}$	0.001339	0.002466	0.012255	0.001210	0.001786	0.003623
$\Xi^{SLCA}$	0.001704	0.002673	0.126436	0.002404	0.001961	0.004168
$\Xi^{ALCA}$	0.003005	0.002762	0.009604	0.003734	0.004742	0.005744
$\Xi^{LP}$	0.001254	0.001080	0.002911	0.002929	0.002804	0.002284
$\Xi^{BJ}$	0.003822	0.003155	0.007410	0.007574	0.007564	0.006928
$\Xi^{mwc}$	0.000813	0.000616	0.002621	0.000817	0.001313	0.001416
2-step (I)	0.001386	0.000902	0.003950	0.001365	0.002363	0.002285
2-step (II)	0.001243	0.000720	0.003251	0.001201	0.002218	0.001951
2-step (III)	0.001701	0.001081	0.005111	0.001641	0.002835	0.002776

TABLE VI: Standard deviation of table II

	$\sigma[K(\mathbf{C}, \Xi_i)]$	$\sigma[K(\mathbf{C}^{-1}, \Xi_i^{-1})]$	$\sigma[F(\mathbf{C}, \Xi_i)]$	$\sigma[F(\mathbf{C}^{-1}, \Xi_i^{-1})]$	$\sigma[MV(\mathbf{C}, \Xi_i)]$	$\sigma[SS(\mathbf{C}, \Xi_i)]$
$\Xi^{naive}$	0.033590	0.006257	0.029705	0.839826	0.045949	0.038741
$\Xi^{linear}$	0.025344	0.010312	0.060261	0.219508	0.022980	0.035558
$\Xi^{RMT}$	0.003561	0.001478	0.028788	0.003255	0.004631	0.004512
$\Xi^{SLCA}$	0.008248	0.003570	0.409100	0.012593	0.006462	0.011566
$\Xi^{ALCA}$	0.003220	0.003052	0.029532	0.006385	0.003609	0.006234
$\Xi^{LP}$	0.001856	0.001735	0.031662	0.004775	0.002604	0.003466
$\Xi^{BJ}$	0.003616	0.003286	0.036123	0.010320	0.005787	0.006746
$\Xi^{mwc}$	0.001616	0.001463	0.019595	0.002015	0.001756	0.003051
2-step (I)	0.001960	0.001595	0.015716	0.003013	0.002453	0.003531
2-step (II)	0.003166	0.002485	0.038539	0.005073	0.003433	0.005551
2-step (III)	0.002676	0.002115	0.032250	0.004560	0.003188	0.004726

TABLE VII: Standard deviation of table III

	$\sigma[K(\mathbf{C}, \Xi_i)]$	$\sigma[K(\mathbf{C}^{-1}, \Xi_i^{-1})]$	$\sigma[F(\mathbf{C}, \Xi_i)]$	$\sigma[F(\mathbf{C}^{-1}, \Xi_i^{-1})]$	$\sigma[MV(\mathbf{C}, \Xi_i)]$	$\sigma[SS(\mathbf{C}, \Xi_i)]$
$\Xi^{naive}$	0.003077	0.000624	0.001973	0.051478	0.005256	0.003634
$\Xi^{linear}$	0.002358	0.001631	0.004774	0.009869	0.003161	0.003988
$\Xi^{RMT}$	0.000081	0.000080	0.001914	0.000031	0.000094	0.000156
$\Xi^{SLCA}$	0.000509	0.000316	0.266979	0.000170	0.000321	0.000804
$\Xi^{ALCA}$	0.000033	0.000036	0.000884	0.000073	0.000050	0.000068
$\Xi^{LP}$	0.000097	0.000075	0.001979	0.000089	0.000117	0.000168
$\Xi^{BJ}$	0.000517	0.000393	0.002411	0.001740	0.001068	0.000906
$\Xi^{mwc}$	0.000089	0.000083	0.001814	0.000034	0.000095	0.000170
2-step (I)	0.000021	0.000024	0.000936	0.000026	0.000024	0.000045
2-step (II)	0.000052	0.000043	0.002507	0.000040	0.000036	0.000095
2-step (III)	0.000039	0.000035	0.001989	0.000033	0.000030	0.000073

TABLE VIII: Standard deviation of table IV

	$\sigma[K(\mathbf{C}, \Xi_i)]$	$\sigma[K(\mathbf{C}^{-1}, \Xi_i^{-1})]$	$\sigma[F(\mathbf{C}, \Xi_i)]$	$\sigma[F(\mathbf{C}^{-1}, \Xi_i^{-1})]$	$\sigma[MV(\mathbf{C}, \Xi_i)]$	$\sigma[SS(\mathbf{C}, \Xi_i)]$
$\Xi^{naive}$	0.006086	0.000649	0.023043	0.150361	0.004538	0.006387
$\Xi^{linear}$	0.008967	0.001170	0.034157	0.181541	0.005588	0.010062
$\Xi^{RMT}$	0.000102	0.000114	0.031821	0.000306	0.000121	0.000211
$\Xi^{SLCA}$	0.000481	0.000364	0.878742	0.001368	0.000099	0.000838
$\Xi^{ALCA}$	0.000066	0.000069	0.022234	0.000290	0.000055	0.000130
$\Xi^{LP}$	0.000119	0.000134	0.033338	0.000395	0.000119	0.000248
$\Xi^{BJ}$	0.000616	0.000526	0.037554	0.003146	0.000993	0.001108
$\Xi^{mwc}$	0.000100	0.000101	0.021536	0.000274	0.000114	0.000200
2-step (I)	0.000071	0.000080	0.020135	0.000290	0.000105	0.000151
2-step (II)	0.000116	0.000132	0.036929	0.000535	0.000110	0.000248
2-step (III)	0.000100	0.000115	0.032987	0.000460	0.000102	0.000215

**Theorem 2** Let  $\mathbf{A} \geq O$  be an irreducible  $n \times n$  matrix. Then,

1.  $\mathbf{A}$  has a positive real eigenvalue equal to its spectral radius.
2. To  $\rho(\mathbf{A})$  there corresponds an eigenvector  $\mathbf{x} \geq 0$ .
3.  $\rho(\mathbf{A})$  increases when any entry of  $\mathbf{A}$  increases.
4.  $\rho(\mathbf{A})$  is a simple eigenvalue of  $\mathbf{A}$ .

**Lemma 1** If  $\mathbf{A} = [a_{ij}] > O$  is an irreducible  $n \times n$  matrix, then either

$$\sum_{j=1}^n a_{ij} = \rho(\mathbf{A}) \quad \text{for all } 1 \leq i \leq n, \quad (\text{B4})$$

or

$$\min_{1 \leq i \leq n} \left( \sum_{j=1}^n a_{ij} \right) < \rho(\mathbf{A}) < \max_{1 \leq i \leq n} \left( \sum_{j=1}^n a_{ij} \right) \quad (\text{B5})$$

**Definition 5** Let  $\mathbf{A}$  be a reducible  $n \times n$  matrix. By definition 2, there exists an  $n \times n$  permutation matrix  $P_1$  such that

$$PAP' = \begin{pmatrix} A_{11} & A_{12} \\ O & A_{22} \end{pmatrix} \quad (\text{B6})$$

where  $A_{11}$  is an  $r \times r$  submatrix and  $A_{22}$  is an  $(n-r) \times (n-r)$  submatrix, with  $1 \leq r < n$ . We ask again if  $A_{11}$  and  $A_{22}$  are irreducible, and if not, we reduce them in the manner we initially reduced the matrix  $A$  in (B6). Thus, there exists an  $n \times n$  permutation matrix  $P$  such that

$$PAP' = \begin{pmatrix} R_{11} & R_{12} & \dots & R_{1m} \\ O & R_{22} & \dots & R_{2m} \\ \vdots & \vdots & \ddots & \vdots \\ O & O & \dots & R_{mm} \end{pmatrix}, \quad (\text{B7})$$

where each submatrix  $R_{ij}$ ,  $1 \leq j \leq m$ , is either irreducible or a  $1 \times 1$  null matrix. We shall say that (B7) is the normal form of a reducible matrix  $\mathbf{A}$ .

**Theorem 3** Let  $\mathbf{A} \geq O$  be an  $n \times n$  matrix. Then,

1.  $\mathbf{A}$  has a nonnegative real eigenvalue equal to its spectral radius. Moreover, this eigenvalue is positive unless  $\mathbf{A}$  is reducible and the normal form of  $A$  is strictly upper triangular.
2. To  $\rho(\mathbf{A})$ , there corresponds a nonzero eigenvector  $\mathbf{x} \geq 0$ .
3.  $\rho(\mathbf{A})$  does not decrease when any entry of  $\mathbf{A}$  is increased.

## 2. Top eigenvalues of diagonal block and hierarchical nested models

### a. Diagonal block model

Consider a block diagonal matrix  $\mathbf{A}$  of dimension  $p \times p$  with  $b$  blocks  $\mathbf{A}_l$  ( $l = 1, \dots, b$ ) each of dimensions  $p_l \times p_l$

satisfying  $\sum_l p_l = p$

$$\mathbf{A} = \begin{pmatrix} \mathbf{A}_1 & 0 & \dots & 0 \\ 0 & \mathbf{A}_2 & \dots & 0 \\ \dots & \dots & \dots & \dots \\ 0 & 0 & 0 & \mathbf{A}_b \end{pmatrix} \quad (\text{B8})$$

Be each block  $\mathbf{A}_l$  of the form

$$\mathbf{A}_l = \begin{pmatrix} 1 & a^{(l)} & \dots & a^{(l)} \\ a^{(l)} & 1 & \dots & a^{(l)} \\ \dots & \dots & \dots & \dots \\ a^{(l)} & a^{(l)} & a^{(l)} & 1 \end{pmatrix}, \quad (\text{B9})$$

where  $a^{(l)} \in [0, 1]$ . The characteristic polynomial of  $\mathbf{A}_l$  is found to be  $\det(\mathbf{A}_l - \lambda \mathbf{I}) = (1 - a^{(l)} - \lambda)^{p_l-1} (1 + (p_l - 1)a^{(l)} - \lambda) = 0$ . Thus, the eigenvalues of the block  $\mathbf{A}_l$  are given by

$$\lambda = \begin{cases} 1 + a^{(l)}(p_l - 1); & \text{with multiplicity } 1 \\ \lambda = 1 - a^{(l)}; & \text{with multiplicity } p_l - 1 \end{cases} \quad (\text{B10})$$

The eigenvalues of  $\mathbf{A}$  are the combined eigenvalues of each block due to the property

$$\det(\mathbf{A} - \lambda \mathbf{I}) = \det(\mathbf{A}_1 - \lambda \mathbf{I}) \dots \det(\mathbf{A}_b - \lambda \mathbf{I}) \quad (\text{B11})$$

Therefore, there are  $b$  eigenvalues of  $\mathbf{A}$  that grow with the dimension of their blocks at the rate  $p_l$ . Consequently,  $b$  eigenvalues are not bounded when  $p \rightarrow \infty$ .

In addition, we can notice that  $\mathbf{A}$  is reducible because there does not exist a directed path between the blocks in the associated directed graph  $G(\mathbf{A})$ , that is,  $G(\mathbf{A})$  is not strongly connected. Nevertheless, each directed subgraph  $G(\mathbf{A}_l)$  is strongly connected given that  $\mathbf{A}_l > O$ . Then, each block matrix  $\mathbf{A}_l$  is irreducible, and we can apply Lemma 1 to find a bound to their spectral radius. Further, the sum of each row of  $\mathbf{A}_l$  is the same, then the minimum and maximum is equal. Hence we have

$$\rho(\mathbf{A}_l) = \sum_{j=1}^{p_l} [a_{ij}]_l = 1 + (p_l - 1)a^{(l)}, \quad (\text{B12})$$

Moreover, theorem 3 assures that  $\mathbf{A}$  has a nonnegative real eigenvalue equal to its spectral radius. Therefore one of the spectral radius  $\rho(\mathbf{A}_l)$ ,  $l = 1, \dots, b$ , is the spectral radius of  $\mathbf{A}$ . It can be corroborated that Eq. B12 coincides with the first part of Eq. B10.

### b. Hierarchical nested model

We have something similar for the hierarchical nested model. In this case, the number of independent blocks is reduced. However, each of them is irreducible by the same argument given above. Let  $\mathbf{A}_k$  be an independent hierarchical nested block, where  $\sum_{k=1}^c p_k = p$  ( $k =$

$1, \dots, c$ ), such that  $c < b$ . In other words, each independent hierarchical block is composed of several overlapping blocks. We have by construction

$$\min_{1 \leq i \leq n} \left( \sum_{j=1}^n [a_{ij}]_k \right) = 1 + (p_k - 1)a^{(k)}, \quad (\text{B13})$$

$$\max_{1 \leq i \leq n} \left( \sum_{j=1}^n [a_{ij}]_k \right) = 1 + p_k(p_k - 1)a^{(k)}, \quad (\text{B14})$$

$$(\text{B15})$$

The minimum is reached when no overlapping exists, and the model is reduced to the diagonal block model. The maximum is reached when each internal block overlaps with each other, and as we can have at most  $p_k$  blocks, a factor  $p_k$  appears. Then, considering Lemma 1, the bounds for the spectral radius of each independent block are

$$1 + (p_k - 1)a^{(k)} < \rho(A_k) < 1 + p_k(p_k - 1)a^{(k)} \quad (\text{B16})$$

Again, theorem 3 assures that  $\mathbf{A}$  has a nonnegative real eigenvalue equal to its spectral radius. Thus, one of the

spectral radius  $\rho(\mathbf{A}_k)$ ,  $k = 1, \dots, c$ , is the spectral radius of  $\mathbf{A}$ . Therefore,  $c$  eigenvalues of  $\mathbf{A}$  grow with the dimension of their blocks at the rate  $p_k$  (at least). Consequently,  $c$  eigenvalues are not bounded when  $p \rightarrow \infty$ .

### c. Observations

We observe that the number of independent blocks in the hierarchical nested model is less than the number in the diagonal block model, i.e.,  $c < b$ . Consequently, the block's size of the former should be bigger to satisfy  $\sum_{k=1}^c p_k = \sum_{l=1}^b p_l = p$ . Therefore,  $p_k > p_l$ , and the top eigenvalue of the hierarchical nested model grows faster than the top eigenvalue of the diagonal block model.

In our models  $a^{(k)} = a^{(l)} = \gamma^2 = (0.3)^2 = 0.01$ , the diagonal block model has  $b = 12$  diagonal blocks, while the hierarchical nested model has  $c = 3$  independent (non-overlapping) blocks. Then, it is clear that the top eigenvalue of the latter grows faster to infinity than the former as  $p \rightarrow \infty$ .

- 
- [1] V. A. Marčenko and L. A. Pastur, Distribution of eigenvalues for some sets of random matrices, *Mathematics of the USSR-Sbornik* **1**, 457 (1967).
  - [2] J. Bun, J.-P. Bouchaud, and M. Potters, Cleaning large correlation matrices: tools from random matrix theory, *Physics Reports* **666**, 1 (2017).
  - [3] M. Tumminello, F. Lillo, and R. N. Mantegna, Kullback-leibler distance as a measure of the information filtered from multivariate data, *Physical Review E* **76**, 031123 (2007).
  - [4] M. Tumminello, F. Lillo, and R. N. Mantegna, Hierarchically nested factor model from multivariate data, *EPL (Europhysics Letters)* **78**, 30006 (2007).
  - [5] L. Laloux, P. Cizeau, J.-P. Bouchaud, and M. Potters, Noise dressing of financial correlation matrices, *Physical review letters* **83**, 1467 (1999).
  - [6] V. Plerou, P. Gopikrishnan, B. Rosenow, L. A. N. Amaral, T. Guhr, and H. E. Stanley, Random matrix approach to cross correlations in financial data, *Physical Review E* **65**, 066126 (2002).
  - [7] I. M. Johnstone, On the distribution of the largest eigenvalue in principal components analysis, *The Annals of statistics* **29**, 295 (2001).
  - [8] C. Stein, Estimation of a covariance matrix, in *39th Annual Meeting IMS, Atlanta, GA, 1975* (1975).
  - [9] O. Ledoit and M. Wolf, A well-conditioned estimator for large-dimensional covariance matrices, *Journal of multivariate analysis* **88**, 365 (2004).
  - [10] O. Ledoit and S. P     , Eigenvectors of some large sample covariance matrix ensembles, *Probability Theory and Related Fields* **151**, 233 (2011).
  - [11] O. Ledoit and M. Wolf, Numerical implementation of the quest function, *Computational Statistics & Data Analysis* **115**, 199 (2017).
  - [12] O. Ledoit and M. Wolf, Analytical nonlinear shrinkage of large-dimensional covariance matrices, *The Annals of Statistics* **48**, 3043 (2020).
  - [13] Z. Burda and A. Jarosz, Cleaning large-dimensional covariance matrices for correlated samples, *Physical Review E* **105**, 034136 (2022).
  - [14] M. Tumminello, F. Lillo, and R. N. Mantegna, Shrinkage and spectral filtering of correlation matrices: a comparison via the kullback-leibler distance, *Acta Polonica B* **38** (2007).
  - [15] G. Biroli, J.-P. Bouchaud, and M. Potters, The student ensemble of correlation matrices: eigenvalue spectrum and kullback-leibler entropy, *Acta Physica Polonica B* **38**, 4009 (2007).
  - [16] O. Ledoit and M. Wolf, Shrinkage estimation of large covariance matrices: Keep it simple, statistician?, *Journal of Multivariate Analysis* **186**, 104796 (2021).
  - [17] J. A. Mingo and R. Speicher, *Free probability and random matrices*, Vol. 35 (Springer, 2017).
  - [18] M. Potters and J.-P. Bouchaud, *A First Course in Random Matrix Theory: For Physicists, Engineers and Data Scientists* (Cambridge University Press, 2020).
  - [19] Z. Burda, J. Jurkiewicz, and B. Wa     , Spectral moments of correlated wishart matrices, *Physical Review E* **71**, 026111 (2005).
  - [20] Z. Burda, A. Jarosz, M. A. Nowak, J. Jurkiewicz, G. Papp, and I. Zahed, Applying free random variables to random matrix analysis of financial data. part i: The gaussian case, *Quantitative Finance* **11**, 1103 (2011).
  - [21] D. Bartz, Cross-validation based nonlinear shrinkage, *arXiv preprint arXiv:1611.00798* (2016).
  - [22] J. Bun, J.-P. Bouchaud, and M. Potters, Overlaps be-

- tween eigenvectors of correlated random matrices, Physical Review E **98**, 052145 (2018).
- [23] M. R. Anderberg, *Cluster analysis for applications: probability and mathematical statistics: a series of monographs and textbooks*, Vol. 19 (Academic press, 2014).
  - [24] O. Ledoit and M. Wolf, Optimal estimation of a large-dimensional covariance matrix under stein's loss, Bernoulli **24**, 3791 (2018).
  - [25] R. F. Engle, O. Ledoit, and M. Wolf, Large dynamic covariance matrices, Journal of Business & Economic Statistics **37**, 363 (2019).
  - [26] M. M. L. de Prado, *Machine learning for asset managers* (Cambridge University Press, 2020).
  - [27] Z.-D. Bai and J. W. Silverstein, No eigenvalues outside the support of the limiting spectral distribution of large-dimensional sample covariance matrices, The Annals of Probability **26**, 316 (1998).
  - [28] O. Ledoit and M. Wolf, The power of (non-) linear shrinking: A review and guide to covariance matrix estimation, Journal of Financial Econometrics **20**, 187 (2022).
  - [29] R. S. Varga, *Matrix Iterative Analysis*, 2nd ed. (Springer-Verlag, Berlin, 2000).